Numerical Simulation of Electromagnetic and Thermal Stress in REBaCuO Superconducting Ring and Disk Bulks Reinforced by Stainless Steel Ring With Various Widths During Field-Cooled Magnetization

Keita Takahashi, Hiroyuki Fujishiro, Tomoyuki Naito, Yousuke Yanagi, Yoshitaka Itoh, and Takashi Nakamura

***Abstract*—The mechanical stress of the electromagnetic hoop stress, $\sigma_\theta^{\mathrm{FCM}}$, during field-cooled magnetization (FCM) from 20 T, and the thermal hoop stress, $\sigma_\theta^{\mathrm{cool}}$, under cooling, in REBaCuO disk and ring bulks reinforced by stainless steel (SUS) ring with various widths, were calculated using numerical simulations. The reinforcement effect of the SUS ring was investigated for each bulk. For the ring bulk, the maximum of $\sigma_\theta^{\mathrm{FCM}}$ was reduced with increasing SUS ring width, from 216 MPa for without SUS ring reinforcement, down to 93 MPa for using SUS ring with 20 mm in width, was less than that of the disk bulk. The numerical results showed that the stress concentration in the ring bulk could be alleviated by the SUS ring reinforcement. We suggest that the width of SUS ring needs to be at least 10 mm to prevent the fracture behavior of the bulk. The optimal design of the reinforcement ring should be constructed so that the total hoop stress, $\sigma_\theta^{\mathrm{total}}$ $(= \sigma_\theta^{\mathrm{FCM}} + \sigma_\theta^{\mathrm{cool}})$, could be less than the fracture strength of the bulk during FCM.**

***Index Terms*—Bulk superconductors, finite-element method, mechanical strength, numerical simulation, trapped field magnets.**

I. Introduction

REBACUO BULK superconductors (RE: rare earth element or Y) have a capability to be a compact and strong magnetic field source as a trapped field magnets (TFMs), which have been shown to trap a magnetic field over 17 T in a GdBaCuO disk bulk pair reinforced using shrink-fit stainless steel by field-cooled magnetization (FCM) [1]. Ring shaped bulks with a concentric hole are also considered to be used as a TFM for practical applications such as nuclear magnetic resonance (NMR) spectrometer [2] and magnetic resonance imaging (MRI) apparatus [3]. Contrary to the superiority, TFMs are broken in the higher magnetic field during FCM by Lorentz force due to the current-field interaction. During its magnetization, the principal hoop stress exceeds the fracture strength, and cracks propagate the radial direction of the bulk [4]. The fracture strength of REBaCuO bulk is reported to be ∼50 MPa along the circumferential direction [5], and could be enhanced to 70 MPa by silver (Ag) addition [6]–[8]. Particularly, in the ring bulk, the hoop stress concentrates at the inner edge of concentric hole, where the actual hoop stress is enhanced twice as high as that of the disk bulk [9], and the bulk could break easier [10]. Numerical analysis is an effective way to understand the mechanical behavior in the bulk during FCM. However, most of those considerations have been based on a numerical equation for the infinite bulk with Bean's model ever [11]–[14]. Recently, we reported the numerical results of mechanical stresses during FCM in the finite height REBaCuO ring bulk reinforced by a metal ring [15]. The fracture strength of the ring bulk could be estimated using the simulation combined with an actual experimental result [16]. As a typical reinforcement technique, a metal ring has been used commonly [1], [2]. However, the reinforcement effect of such metal ring has not been investigated extensively, except for a conventional setup.

In this paper, we compared the numerical results of the mechanical stresses; the electromagnetic hoop stress, $\sigma_\theta^{\mathrm{FCM}}$, during FCM from 20 T and the thermal hoop stress, $\sigma_\theta^{\mathrm{cool}}$, under cooling from 300 K to 50 K, in the finite height REBaCuO disk and ring shaped bulks reinforced by a stainless steel (SUS) ring with various widths. It is shown that the stress concentration in the ring bulk could be abbreviated to the same level as that of the disk bulk using wider stainless steel ring.

II. Numerical Simulation Framework

To discuss the mechanical behavior during the magnetization, we constructed the following framework of three-dimensional numerical model. Fig. 1 presents schematic view of numerical

Manuscript received August 23, 2017; accepted January 22, 2018. Date of publication January 30, 2018; date of current version February 20, 2018. This work was supported in part by the "Development of Systems and Technologies for Advanced Measurement and Analysis" from Japan Agency for Medical Research and Development (AMED), and in part by the JSPS KAKENHI under Grant 15K04646. *(Corresponding author: Keita Takahashi.)*

K. Takahashi, H. Fujishiro, and T. Naito are with the Department of Physical Science and Materials Engineering, Faculty of Science and Engineering, Iwate University, Morioka 020-8551, Japan (e-mail: t0212032@iwate-u.ac.jp; fujishiro@iwate-u.ac.jp; tnaito@iwate-u.ac.jp).

Y. Yanagi and Y. Ito are with the IMRA Material R&D Company Ltd., Kariya 448-0032, Japan (e-mail: yanagi@ai-i.aisin.co.jp; y-itoh@ai-i.aisin.co.jp).

T. Nakamura is with RIKEN, Wako 351-0198, Japan (e-mail: takashi.nakamura@riken.jp).

Color versions of one or more of the figures in this paper are available online at http://ieeexplore.ieee.org.

Digital Object Identifier 10.1109/TASC.2018.2799578

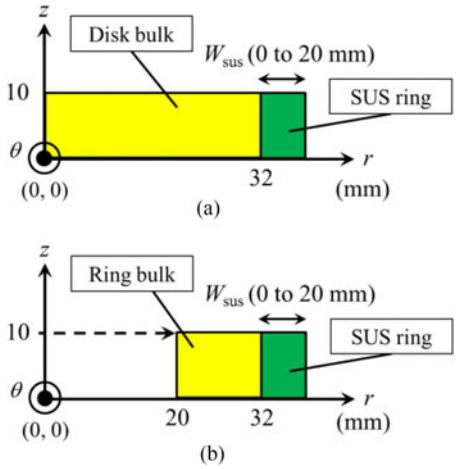

Fig. 1. Schematic view of numerical models for (a) the disk bulk and (b) the ring bulk.

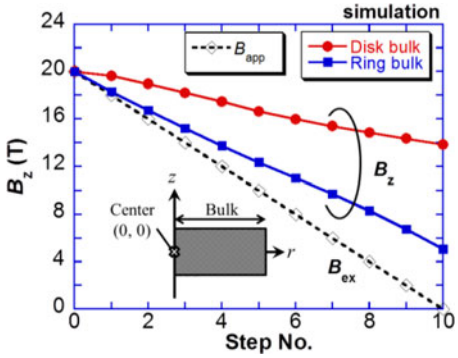

Fig. 2. Time step dependence of the trapped field, B_z, at the center of each bulk for the disk bulk and the ring bulk during FCM from $B_{app} = 20$ T.

TABLE I
MECHANICAL PARAMETERS USED IN THE NUMERICAL SIMULATION.

	E (GPa)	ν	α (K^{-1})
REBaCuO bulk	100	0.33	5.2e-6
SUS316L	193	0.28	1.27e-5

(E: Young's modulus, ν: Poisson ratio, α: thermal expansion coefficient.)

half models ($z \geq 0$) for (a) the disk bulk (64 mm in O.D., 20 mm in height), and (b) the ring bulk (40 mm in I.D., 64 mm in O.D., 20 mm in height). Each bulk was reinforced by a stainless steel (SUS316L) ring holder of the same height as the bulk with various widths of 0 mm (without SUS ring), 5 mm, 10 mm or 20 mm in radial direction to compare the reinforcement effect for each bulk. We abbreviate the width of SUS ring like as $W_{SUS} = 5$ mm, which is a conventional width used in actual apparatus [2], [16].

Each bulk was magnetized by FCM using an infinite solenoid coil (120 mm I.D., 170 mm O.D. and infinite height). Physical phenomena during FCM are described using an electromagnetic equation based on the axisymmetric coordinate system [17], [18], in which the temperature of the REBaCuO bulks is assumed to be constant at $T_s = 50$ K during FCM for simplicity. The power-n law ($n = 20$) was used to describe the nonlinear E–J characteristic of the bulk [19]. The magnetic field dependence of critical current density, $J_c(B)$, of the bulk was described using the following equation [20], [21].

$$J_c(B) = J_{c1} \exp\left(-\frac{B}{B_L}\right) + J_{c2}\frac{B}{B_{max}} \times \exp\left[\frac{1}{k}\left(1 - \left(\frac{B}{B_{max}}\right)^k\right)\right]. \quad (1)$$

J_{c1} was supposed to be 8.0×10^8 A/m^2, which was a rational value as to reproduce the actual experimental results of the trapped field during FCM at 50 K [16]. In FCM process, a magnetic field of $B_{app} = 20$ T was applied above the critical temperature, T_c (= 92 K), and then the bulk was cooled to $T_s = 50$ K. Then, the magnitude of the magnetic field was decreased linearly from 20 T to zero in 10 steps, as shown in Fig. 2. Elastic behavior of an isotropic material can be explained by Hooke's law, in which the stress is linearly proportional to the strain [15]. The electromagnetic hoop stress, σ_θ^{FCM}, was estimated for each step of FCM, which acts circumferentially on each end face of the meshed element [11], [12]. The thermal hoop stress, σ_θ^{cool}, by cooling from 300 K to 50 K was also calculated for each model. Table I summarizes the mechanical parameters (Young's modulus, E, Poisson ratio, ν, and thermal expansion coefficient, α) of the REBaCuO bulk and the SUS ring. The REBaCuO bulk is assumed to be not broken with an isotropic and homogeneous properties for simplicity. Commercial software, Photo-Eddy and Photo-ELAS (Photon Ltd., Japan), were used for analyses of electromagnetic properties and mechanical stresses.

III. RESULTS AND DISCUSSION

A. Trapped Field, B_z, and Lorentz Force, F_r

Fig. 2 shows the time step dependence of the trapped field, $B_z(t)$, at the center $(r, z) = (0, 0)$ of each bulk. $B_z(t)$ gradually decreased with increasing time step, and settled in a certain value of the trapped field, B_T, at the final step after FCM; $B_T = 13.8$ T for the disk bulk and $B_T = 5.1$ T for the ring bulk. We confirmed that the induced current flowed in the whole area of each bulk, showing that the applied field is sufficient to magnetize the bulk fully.

Fig. 3 shows the contour maps of the Lorentz force density along r-direction, F_r ($= B_z \times J_\theta$), at each time step of 2, 6 and 10 for the disk bulk (a)∼(c), and for the ring bulk (d)∼(f). Note that the Lorentz force was not applied to the SUS ring due to $J_\theta = 0$. In Fig. 3(a) and (d), in the early stage at step 2, F_r was applied mainly on the outside of the bulk because the induced current starts to flow from the outer side of the bulk. However, the magnitude of F_r is relatively low at step 2.

In Fig. 3(b) and (e), F_r was enhanced in the whole region of each bulk with progress of FCM due to the current-field interaction between B_z and J_θ. After FCM, in Fig. 3(c) and (f), F_r turned on a negative value at the outside of the bulk

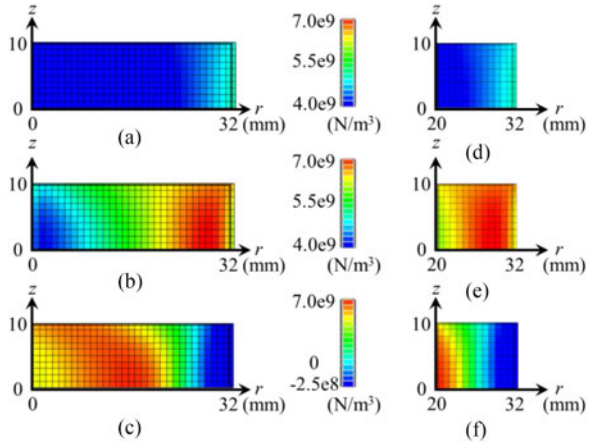

Fig. 3. Contour maps of Lorentz force density along r-direction, F_r, $(= B_y \times J_\theta)$ at each time step of (a) Step 2, (b) Step 6 and (c) Step 10 for the disk bulk, and (d) Step 2, (e) Step 6 and (f) Step 10 for the ring bulk. The SUS ring was supposed to be as a non-magnetic material and not involved here.

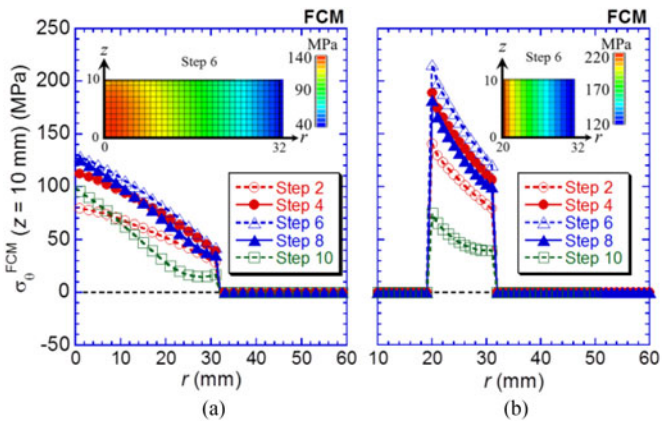

Fig. 4. Time step dependence of cross-sectional plots of the electromagnetic hoop stress, $\sigma_\theta^{\rm FCM}$, along r-direction on the bulk surface ($z = 10$ mm) without SUS ring reinforcement during FCM for (a) the disk bulk and (b) the ring bulk. The contour maps of $\sigma_\theta^{\rm FCM}$ at step 6 are also shown in each panel. (a) Disk bulk. (b)Ring bulk.

because the magnetic flux lines sneak around there to build a conical-shaped trapped field profile.

B. Electromagnetic Hoop Stress, σ_θ^{FCM} During FCM

Fig. 4 shows the time step dependence of cross-sectional plots of the electromagnetic hoop stress, $\sigma_\theta^{\rm FCM}$, along r-direction on the bulk surface ($z = 10$ mm) without SUS ring reinforcement during FCM for each bulk. The contour maps of $\sigma_\theta^{\rm FCM}$ at step 6 are also shown in each panel. For the disk bulk in Fig. 4(a), $\sigma_\theta^{\rm FCM}$ had a peak value of $+130$ MPa in the center of the bulk ($r = 0$ mm) at step 6 during FCM. Similar behavior was confirmed for the ring bulk in Fig. 4(b), but the maximum of $\sigma_\theta^{\rm FCM}$ was $+216$ MPa at step 6 due to the stress concentration at the inner periphery ($r = 20$ mm), is much larger than that of the disk bulk. The contour maps show that $\sigma_\theta^{\rm FCM}$ profile is relatively homogeneous along z-direction of the bulk.

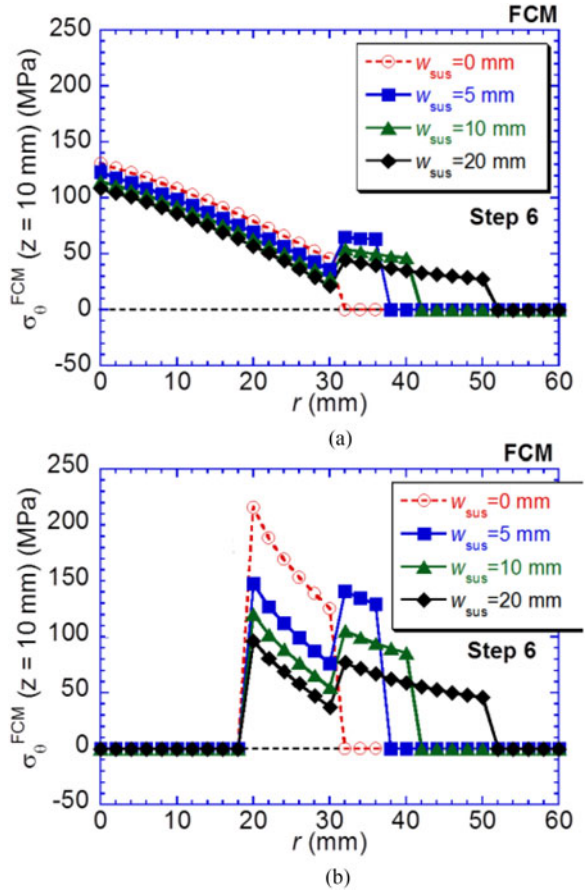

Fig. 5. Cross-sectional plots of the electromagnetic hoop stress, $\sigma_\theta^{\rm FCM}$, along r-direction on the bulk surface ($z = 10$ mm) reinforced by SUS ring with various widths at step 6 during FCM for (a) the disk bulk and (b) the ring bulk.

Fig. 5 shows the cross-sectional plots of the electromagnetic hoop stress, $\sigma_\theta^{\rm FCM}$, along r-direction on the bulk surface ($z = 10$ mm) reinforced by SUS ring with various widths at step 6 during FCM for each bulk. In Fig. 5(a), $\sigma_\theta^{\rm FCM}$ was reduced with increasing $W_{\rm SUS}$ in the whole area of both the disk bulk and the SUS ring. The maximum $\sigma_\theta^{\rm FCM}$ of the disk bulk was reduced from $+130$ MPa for without SUS ring down to $+108$ MPa for $W_{\rm SUS} = 20$ mm. On the other hand, for the ring bulk in Fig. 5(b), the maximum $\sigma_\theta^{\rm FCM}$ was fairly reduced from $+216$ MPa to $+97$ MPa. These results indicate that the stress concentration in the ring bulk could be alleviated to the same level as the disk bulk. Thus, the reinforcement effect of wider SUS ring is more effective to reduce $\sigma_\theta^{\rm FCM}$ during FCM in the ring bulk.

C. Thermal Hoop Stress, σ_θ^{cool}, Under Cooling

Fig. 6 shows the cross-sectional plots of the thermal hoop stress, $\sigma_\theta^{\rm cool}$, along r-direction on the bulk surface ($z = 10$ mm) reinforced by SUS ring with various widths under cooling from 300 K to 50 K for each bulk. Note that the bulk without SUS ring ($W_{\rm SUS} = 0$ mm) shrink freely, that is, $\sigma_\theta^{\rm cool} = 0$ MPa. We have reported that the difference of the thermal contraction between the ring bulk and the SUS ring might cause a tensile stress under cooling process [11], [12]. Also here, for the case

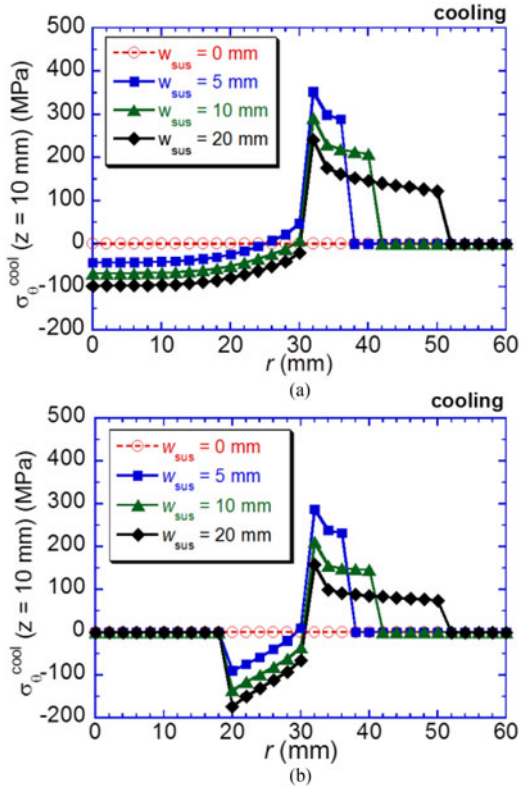

Fig. 6. Cross-sectional plots of the thermal hoop stress, $\sigma_\theta^{\rm cool}$, along r-direction on the bulk surface ($z = 10$ mm) reinforced by SUS ring with various widths under cooling from 300 K to 50 K for (a) the disk bulk and (b) the ring bulk.

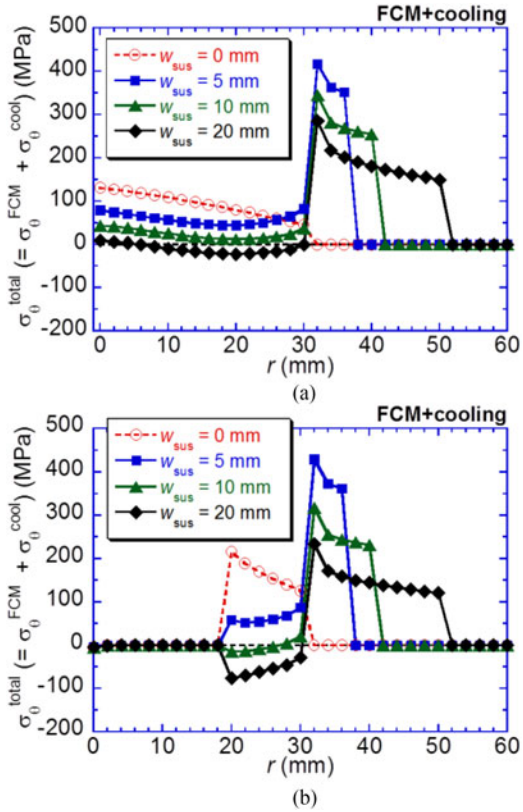

Fig. 7. Cross-sectional plots of the total hoop stress, $\sigma_\theta^{\rm total}$, along r-direction on the bulk surface ($z = 10$ mm) reinforced by SUS ring with various widths for (a) the disk bulk and (b) the ring bulk.

of $W_{\rm SUS} = 5$ mm, $\sigma_\theta^{\rm cool}$ had a maximum value at the outer edge ($r = 32$ mm) of the bulk, +47 MPa in Fig. 6(a), and +10 MPa in Fig. 6(b). These tensile $\sigma_\theta^{\rm cool}$ values were reduced with increasing $W_{\rm SUS}$, which results in a negative value in the whole area of each bulk for $W_{\rm SUS} = 10$, and 20 mm. The reinforcement using wider SUS ring was effective for each bulk under cooling process as well.

D. Total Hoop Stress, σ_θ^{total}, During FCM Under Cooling

To discuss the mechanical behavior of the bulk reinforced by SUS ring in the actual FCM, the total hoop stress, $\sigma_\theta^{\rm total}$ ($= \sigma_\theta^{\rm FCM} + \sigma_\theta^{\rm cool}$) should be considered, including $\sigma_\theta^{\rm FCM}$ and $\sigma_\theta^{\rm cool}$ mentioned in previous subsections. Fig. 7 shows the cross-sectional plots of the total hoop stress, $\sigma_\theta^{\rm total}$, along r-direction on the bulk surface ($z = 10$ mm) reinforced by the SUS ring with various widths, were calculated from Figs. 5 and 6 for each bulk. For the case of $W_{\rm SUS} = 0$ mm, $\sigma_\theta^{\rm FCM}$ was imported as $\sigma_\theta^{\rm total}$ value directly. When the SUS ring with $W_{\rm SUS} = 5$ mm was used for both cases, the tensile $\sigma_\theta^{\rm total}$ higher than +50 MPa is applied, is as high as the fracture strength of the REBaCuO bulk ($\cong 59$ MPa) [16]. The $\sigma_\theta^{\rm total}$ was reduced with increasing $W_{\rm SUS}$, resulting in the minimum value for $W_{\rm SUS} = 20$ mm in the whole region of the bulk and the SUS ring, due to the stress relaxation by the reinforcement effect. These results indicate that the SUS ring alleviates the tensile strain in the bulk during FCM. Meanwhile, under cooling process, the SUS ring enhances the compressive strain to countermeasure $\sigma_\theta^{\rm FCM}$ during FCM. The width of SUS ring needs to be at least 10 mm to prevent the fracture behavior of the bulk in present simulation.

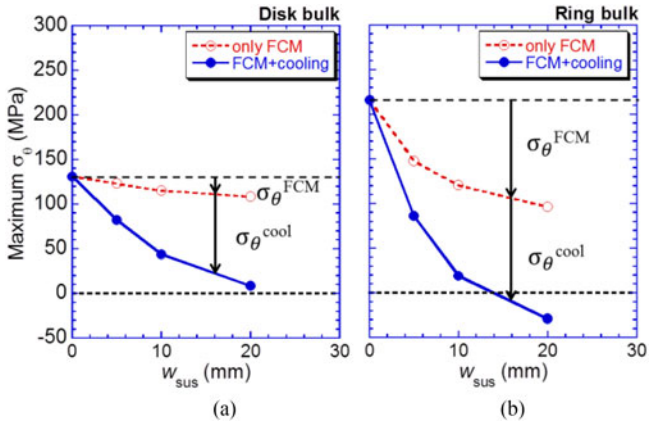

Fig. 8. The SUS ring width, $W_{\rm SUS}$, dependence of the maximum of the electromagnetic hoop stress, $\sigma_\theta^{\rm FCM}$, and the total hoop stress, $\sigma_\theta^{\rm total}$, for (a) the disk bulk and (b) the ring bulk, which were extracted from Figs. 5 and 7, respectively.

Fig. 8 shows the SUS ring width, $W_{\rm SUS}$, dependence of the maximum of the electromagnetic hoop stress, $\sigma_\theta^{\rm FCM}$, during FCM and the total hoop stress, $\sigma_\theta^{\rm total}$, during FCM under cooling,, for each bulk, which were extracted from Figs. 5 and 7. During FCM, the ring bulk was subject to a large maximum

$\sigma_\theta^{\mathrm{FCM}}$ of $+216$ MPa at the inner periphery around the bulk annuli for the case of $W_{\mathrm{SUS}} = 0$, without SUS ring reinforcement, due to the stress concentration as shown in Fig. 8(b). Surprisingly, compared to the disk bulk, $\sigma_\theta^{\mathrm{FCM}}$ during FCM in the ring bulk was more susceptible to the reinforcement effect of wider SUS ring, which results in a lower $\sigma_\theta^{\mathrm{FCM}}$ value at $W_{\mathrm{SUS}} = 20$ mm. A decrease of $\sigma_\theta^{\mathrm{FCM}}$ by the wider SUS ring was within a few MPa in the disk bulk, and that reinforcement effect was fairly small during FCM. On the other hand, under cooling process, it was confirmed that the wider SUS ring was desirable to enhance the compressive stress for each bulk. The achieved lowest $\sigma_\theta^{\mathrm{total}}$ value at $W_{\mathrm{SUS}} = 20$ mm was $+9$ MPa for the disk bulk, and -29 MPa for the ring bulk, respectively. The magnitude of the mechanical stress depends on the magnetizing condition around the bulk, such as geometry, superconducting characteristics of the bulk, and the applied field. An optimal design of the reinforcement ring could be useful to alleviate the magnetic stress, and should be constructed so that the $\sigma_\theta^{\mathrm{total}}$ could be less than the fracture strength of the bulk during FCM.

IV. Summary

In this study, the numerical results of the mechanical stress of the electromagnetic hoop stress, $\sigma_\theta^{\mathrm{FCM}}$, during FCM from 20 T at 50 K, and the thermal hoop stress, $\sigma_\theta^{\mathrm{cool}}$, under cooling, in REBaCuO disk and ring bulks reinforced by SUS ring with various widths, were compared. For the ring bulk, the maximum of $\sigma_\theta^{\mathrm{total}}$ at step 6 during FCM was reduced from $+216$ MPa without SUS ring reinforcement, down to -29 MPa for $W_{\mathrm{SUS}} = 20$ mm, is less than that of the disk bulk. The numerical results showed that the stress concentration in the ring bulk could be alleviated by the wider SUS ring. The width of SUS ring needs to be at least 10 mm to prevent the fracture behavior of the bulk. An optimal design of the reinforcement ring should be constructed so that the total hoop stress, $\sigma_\theta^{\mathrm{total}} (= \sigma_\theta^{\mathrm{FCM}} + \sigma_\theta^{\mathrm{cool}})$, could be less than the fracture strength of the bulk during FCM.

References

[1] J. H. Durrell *et al.*, "A trapped field of 17.6 T in melt-processed, bulk Gd-Ba-Cu-O reinforced with shrink-fit steel," *Surpercond. Sci. Technol.*, vol. 27, 2014, Art. no. 082001.

[2] T. Nakamura *et al.*, "Development of a superconducting bulk magnet for NMR and MRI," *J. Mag. Reson.*, vol. 259, pp. 68–75, 2015.

[3] D. Tamada, T. Nakamura, Y. Itoh, and K. Kose, "Experimental evaluation of the magnetization process in a high T_c bulk superconducting magnet using magnetic resonance imaging," *Physica C*, vol. 492, pp. 174–147, 2013.

[4] T. Miyamoto, K. Nagashima, N. Sakai, and M. Murakami, "Direct measurement of mechanical properties for large-grain bulk superconductors," *Physica C*, vol. 340, pp. 41–50, 2000.

[5] A. Murakami *et al.*, "Mechanical properties of Gd123 bulk superconductors at room temperature," *Cryogenics*, vol. 43, pp. 345–350, 2003.

[6] D. Lee and K. Salama, "Enhancements in current density and mechanical properties of Y-Ba-Cu-O/Ag composites," *Jpn. J. Appl. Phys.*, vol. 29, pp. L2017–L2019, 1990.

[7] M. Matsui, N. Sakai, and M. Murakami, "Effect of Ag_2O addition on the trapped field and mechanical properties of Nd-Ba-Cu-O bulk superconductors," *Surpercond. Sci. Technol.*, vol. 15, pp. 1092–1098, 2002.

[8] K. Katagiri *et al.*, "Effects of Ag content on the mechanical properties of (Nd,Eu,Gd)-Ba-Cu-O bulk superconductors," *Physica C*, vol. 392–396, pp. 526–530, 2003.

[9] T. H. Johansen, C. Wang, Q. Y. Chen, and W. -K. Chu, "Enhancement of tensile stress near a hole in superconducting trapped-field magnets," *J. Appl. Phys.*, vol. 88, pp. 2730–2733, 2000.

[10] H. Mochizuki, H. Fujishiro, T. Naito, Y. Itoh, Y. Yanagi, and T. Nakamura, "Trapped field characteristics and fracture behavior of REBaCuO bulk ring during pulsed field magnetization," *IEEE Trans. Appl. Supercond.*, vol. 26, no. 4, Jun. 2016, Art. no. 6800205.

[11] Y. Ren, R. Weinstein, J. Liu, R. P. Sawh, and C. Foster, "Damage caused by magnetic pressure at high trapped field in quasi-permanent magnets composed of melt-textured Y–Ba–Cu–O superconductor," *Physica C*, vol. 251, pp. 15–26, 1995.

[12] T. H. Johansen, "Flux-pinning-induced stress and strain in superconductors: Case of a long circular cylinder," *Phys. Rev. B*, vol. 60, pp. 9690–9703, 1999.

[13] T. H. Johansen, "Flux-pinning-induced stress and magnetostriction in bulk superconductors," *Supercond. Sci. Technol*, vol. 13, pp. R121–R137, 2000.

[14] W. J. Feng, P. Ma, Q. H. Li, and J. X. Liu, "Flux-pinning-induced magnetostriction and stress in a transversely isotropic thin superconducting disk with a concentric small hole," *J. Supercond. Novel Magn.*, vol. 26, pp. 539–543, 2013.

[15] H. Fujishiro *et al.*, "Simulation studies of mechanical stresses in REBaCuO superconducting ring bulks with infinite and finite height reinforced by metal ring during field-cooled magnetization," *Supercond. Sci. Technol.*, vol. 30, 2017, Art. no. 085008.

[16] K. Takahashi, H. Fujishiro, T. Naito, Y. Yanagi, Y. Itoh, and T. Nakamura, "Fracture behavior analysis of EuBaCuO superconducting ring bulk reinforced by a stainless steel ring during field-cooled magnetization," *Supercond. Sci. Technol.*, vol. 30, 2017, Art. no. 115006.

[17] H. Fujishiro and T. Naito, "Simulation of temperature and magnetic field distribution in superconducting bulk during pulsed field magnetization," *Supercond. Sci. Technol.*, vol. 23, 2011, Art. no. 105021.

[18] H. Fujishiro, H. Mochizuki, M. D. Ainslie, and T. Naito, "Trapped field of 1.1 T without flux jumps in an MgB_2 bulk during pulsed field magnetization using a split coil with a soft iron yoke," *Supercond. Sci. Technol.*, vol. 29, 2016, Art. no. 084001.

[19] M. D. Ainslie and H. Fujishiro, "Modelling of bulk superconductor magnetization," *Supercond. Sci. Technol.*, vol. 28, 2015, Art. no. 053002.

[20] M. Jirsa, L. Půst, D. Dlouhý, and M. R. Koblischka, "Fishtail shape in the magnetic hysteresis loop for superconductors: Interplay between different pinning mechanisms," *Phys. Rev. B*, vol. 55, pp. 3276–3284, 1997.

[21] M. Muralidhar, N. Sakai, M. Jirsa, N. Koshizuka, and M. Murakami, "Direct observation and analysis of nanoscale precipitates in $(Sm,Eu,Gd)Ba_2Cu_3O_y$," *Appl. Phys. Lett.*, vol. 85, pp. 3504–3506, 2004.